Int. J. Multiphase Flow Vol. 18, No. 5, pp. 727–738, 1992
Printed in Great Britain.

0301-9322/92 $5.00 + 0.00

A MODEL INVOLVING BREAK-UP TO EXPLAIN PECULIARITIES OF THE BOILING LIQUID EFFLUX PROCESS

O. E. IVASHNIOV and K. I. SOPLENKOV
Department of Biophysics, Biological Faculty, Lomonosov Moscow State University, 119899 Moscow, Russia

(Received 27 June 1990; in revised form 6 February 1992)

Abstract—The opening of a high-pressure vessel, in the form of a closed cylinder which is initially occupied by subcooled water, is considered. At time zero one end of the tube is opened and the liquid starts to flow out. As the atmospheric pressure is less than the liquid saturation pressure, the liquid efflux is accompanied by boiling. A mathematical model of the liquid boiling is proposed which takes into consideration two vaporization mechanisms: (1) the boiling on admixtured particles in the liquid; and (2) the break-up of bubbles. For realization of the second mechanism, a definite correlation between the bubble dimension and the difference in the phase velocities must be attained. Using this model, an unusual wave process, found previously experimentally, is described successfully, i.e. a "slow" wave of discharge, which in spreading along the non-equilibrium two-phase mixture transfers it into a state of equilibrium. Earlier known models of boiling liquid failed to explain the appearance of this wave.

Key Words: bubble break-up, boiling liquid efflux

1. INTRODUCTION

To calculate power construction safety systems it is necessary to determine precisely the parameters of the process of the efflux of boiling liquid from vessels. Much experimental material on such processes has been accumulated. Many authors compare their calculations with the experiments of Edwards & O'Brien (1970). A working section of Edwards & O'Brien's experimental plant was in the form of a closed cylinder of length 4.1 m and 0.073 m dia. The cylinder was initially occupied by subcooled water with temperature $T_0 = 515$ K and at pressure $p_0 = 6.9$ MPa. Liquid of such a temperature starts boiling under the saturation pressure $p_s(T_0) = 0.5p_0$. At time zero, a glass disk which closed the right-hand end of the cylinder was destroyed (the destruction time was $< 10^{-3}$ s). As the atmospheric pressure was less than the liquid saturation pressure, the liquid efflux was accompanied by boiling.

Pressure oscillograms measured at different points of the tube are shown in figure 1(a). The pressure and volumetric vapour fraction oscillograms measured in the cross-section at a distance of 1.39 m from the closed cylinder end are shown in figure 1(a) by the solid line. The volumetric vapour fraction was measured by examination with γ-rays. In experimental oscillograms, a "slow" wave of discharge spreading along the boiling liquid with a speed of the order of 10 m/s is clearly seen. An analogous wave configuration has been observed in a boiling CO_2 efflux investigation (Isaev 1980).

In spite of the fact that the existence of this "slow" wave has been known for over 20 years, the mechanism of its appearance remains unclear.

Current models for the description of boiling liquid flows can be divided into two types. The first type is a model of shock boiling (Labuntzov & Avdeev 1981). It is considered that, after opening of the vessel, a discharge wave of $p_0 - p_*$ amplitude, where $p_* < p_s(T_0)$ is the model free parameter, enters the vessel at the speed of sound in a pure liquid. Then through a metastable liquid, where superheats are $p_s(T_0) - p_*$, moves a shock wave of discharge, in which the liquid starts to boil, i.e. a "slow" wave is viewed as a shock wave. Such a model allows one to obtain sufficient agreement with experiments. However, applying the model of shock boiling to the given flow description [see figure 2a,b)], it is predicted that the liquid near the closed tube side should stay in a subheated state without starting to boil for 0.3 s (until the "slow" wave arrives) and, in the case of a longer channel, for an even longer time, in variance with modern views of boiling

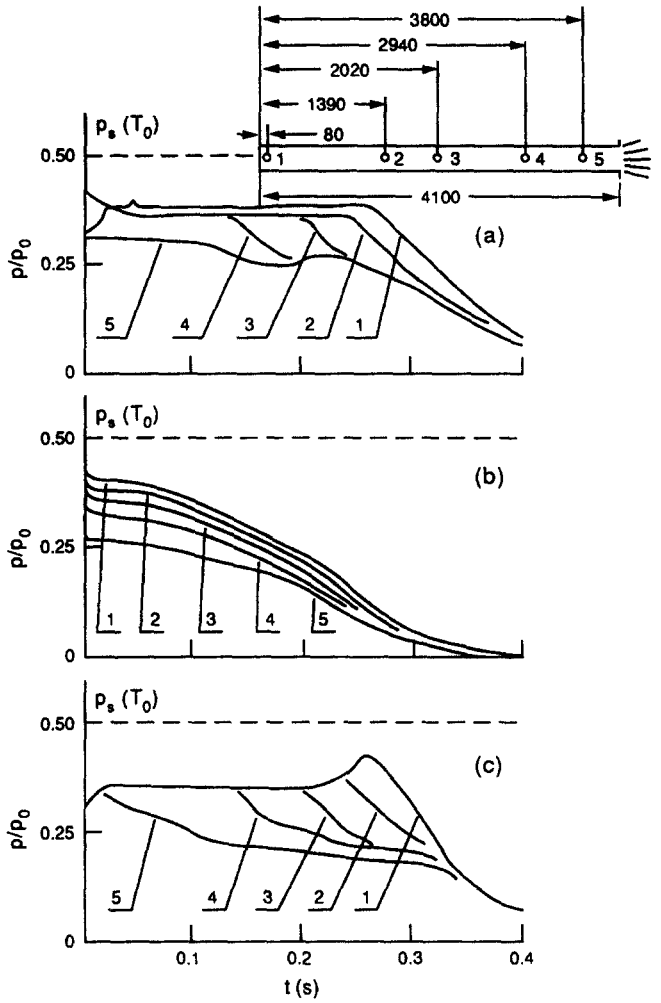

Figure 1. Pressure oscillograms at various tube cross-sections (the locations of which are shown in the insert): (a) experiment (Edwards & O'Brien 1970); (b) calculation with the help of the one-velocity model (Nigmatulin & Soplenkov 1980); (c) calculation with the help of the advanced model.

liquid properties. Secondly, the model of shock boiling fails to explain the experimental fact that the liquid starts to boil [figure 2(b)] before the "slow" wave arrives.

The second type of model can be called a "kinetic" one. The main consideration of such an approach is the modelling of liquid features. Boiling is assumed to begin on admixtured particles when the pressure decreases to the saturation pressure. In the non-equilibrium model (Nigmatulin & Soplenkov 1980), the particle concentration is selected according to calculations corresponding to the experiment. In the equilibrium model (Ivandaev & Gubaidullin 1978), the admixtured particles concentration is assumed infinitely large, and therefore, the liquid and vapour phases are considered always to be in equilibrium.

Pressure oscillograms in the five channel cross-sections obtained with the use of the non-equilibrium model (Nigmatulin & Soplenkov 1980) are shown in figure 1(b). It can see that calculations based on this model misrepresent the flow character. In figure 2(a,b) the theoretical pressure and volumetric vapour content oscillograms at the cross-section $z = 1.39$ m are compared with the experimental ones. The experimental curves are shown by the solid line. Curves calculated on equilibrium (Ivandaev & Gubaidullin 1978) and non-equilibrium (Nigmatulin & Soplenkov 1980) models are shown by the dashed and dotted lines, respectively. An equilibrium model does not describe the drop in pressure below the saturation line. The non-equilibrium model (Nigmatulin & Soplenkov 1980) describes the drop in the pressure but does not explain the appearance of the

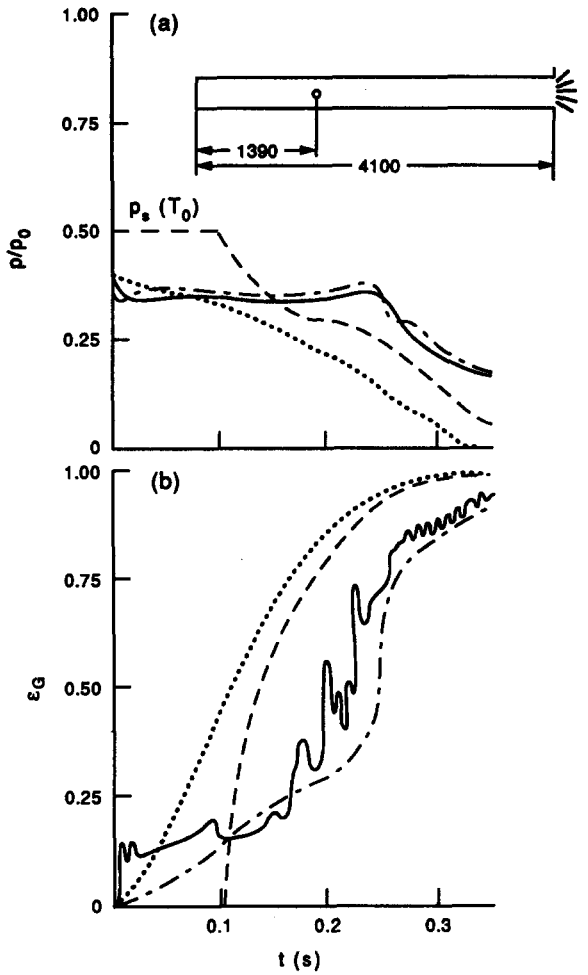

Figure 2. Oscillograms of the pressure (a) and the volumetric vapour content (b) at the cross-section 1.39 m from the closed end of the tube: ——, experiment; – – – –, equilibrium model; · · · ·, non-equilibrium model without bubble break-up; — · —, advanced model.

"slow" wave. A search for new physical representations of the liquid boiling process was necessary in order to understand the reasons leading to the formation of the "slow" discharge wave.

2. MODEL OF BOILING LIQUID FLOW

The hypothesis is advanced in this paper that, in addition to the earlier known vaporization mechanism consisting of a heat growth of bubbles formed on admixtured particles, there is another mechanism—bubble break-up. A necessary condition for this mechanism to be realized is that a definite correlation of the difference in the phase velocities and the bubble dimension is attained. For verification of the proposed hypothesis, a mathematical model was composed. The following assumptions were made under this model:

(1) Boiling was assumed to take place on admixtured particles in the liquid. The number of particles that nucleate boiling per unit of the volume was assumed to be the same ($n_0 = 10^8\ \mathrm{m}^{-3}$) as in calculations on the model (Nigmatulin & Soplenkov 1980).
(2) The pressures in the phases were assumed to be equal.
(3) The parameters in a bubble were considered uniform and equal to those on the saturation line.

(4) The difference in the phase velocities was assumed to be much less than the flow speed.

Taking into consideration the above assumptions, the system of equations for a two-phase mixture can be written. The equations for conservation of mass for the mixture and gas phase are

$$\frac{\partial \rho}{\partial t} + \frac{\partial [\rho u]}{\partial z} = 0 \qquad [1]$$

and

$$\frac{\partial [\rho_G \epsilon]}{\partial t} + \frac{\partial [\rho_G \epsilon u]}{\partial z} = jn, \qquad [2]$$

where: $\rho = \rho_L(1-\epsilon) + \rho_G \epsilon$ is the mixture density, ρ_L and ρ_G are the liquid and gas densities, respectively; ϵ is the volumetric vapour fraction;

$$u = u_L + \frac{\rho_G \epsilon}{\rho}(u_G - u_L)$$

is the velocity of the centre of mass (the mixture velocity) which is equal, on the grounds of assumption (4), to the liquid velocity ($u = u_L$); u_L and u_G are the liquid and gas velocities, respectively; j is the intensity of the liquid vaporization into a bubble; and n is the number of bubbles per unit mixture volume.

The equation for conservation of momentum of the mixture is

$$\frac{\partial [\rho u]}{\partial t} + \frac{\partial [\rho u^2 + p]}{\partial z} = 0, \qquad [3]$$

where p is the pressure.

The equation for conservation of energy of the mixture is

$$\frac{\partial \left[\rho\left(i + \frac{u^2}{2}\right) - p\right]}{\partial t} + \frac{\partial \left[\rho u\left(i + \frac{u^2}{2}\right)\right]}{\partial z} = 0, \qquad [4]$$

where

$$i = \frac{\rho_L(1-\epsilon)}{\rho} i_L + \frac{\rho_G \epsilon}{\rho} i_G$$

is the enthalpy of the mixture and i_L and i_G are the liquid and gas enthalpies, respectively.

The equation for the number of bubbles is

$$\frac{\partial n}{\partial t} + \frac{\partial [nu]}{\partial z} = \psi, \qquad [5]$$

where ψ is the intensity of the bubble break-up.

The equation for conservation of momentum of the bubbles is

$$\rho_G \tfrac{4}{3} \pi a^3 \left(\frac{\partial u_G}{\partial t} + u \frac{\partial u_G}{\partial z}\right) = f_A + f_m + f_\mu, \qquad [6]$$

where a is the bubble radius and f_A, f_m and f_μ are the interfacial forces of Archimedes (buoyancy), virtual mass and drag, respectively.

From assumption (4), the system of equations [1]–[6] lacks terms characterizing the mass, impulse and energy change in a volume moving with a mean mass velocity (u), due to the withdrawal from this volume of the portion of bubbles and liquid whose velocities are not equal to the velocity of the centre of mass. The difference in the phase velocities is considered to affect only the process of bubble break-up.

The force or Archimedes (buoyancy) is given by

$$f_A = \rho_L \tfrac{4}{3} \pi a^3 \left(\frac{\partial u}{\partial t} + u \frac{\partial u}{\partial z}\right). \qquad [7]$$

The virtual mass force is defined as

$$f_m = \frac{\rho_L}{2}\frac{4}{3}\pi a^3\left\{\left(\frac{\partial u}{\partial t}+u\frac{\partial u}{\partial z}\right)-\left(\frac{\partial u_G}{\partial t}+u\frac{\partial u_G}{\partial z}\right)-3(u_G-u)\left[\frac{1-\epsilon}{a}\left(\frac{\partial a}{\partial t}+u\frac{\partial a}{\partial z}\right)+\frac{\epsilon j}{4\pi a^3\rho_L}\right]\right\}. \quad [8]$$

The expression for the interfacial drag force is

$$f_\mu = \frac{c_\mu}{2}\rho_L\pi a^2(u-u_G)|u-u_G|. \quad [9]$$

An expression for the interfacial drag coefficient is obtained by extrapolation of c_μ dependences from Reynolds numbers derived by Adamar-Riybchinskii and Moore (Batchelor 1970) up to their intersection:

$$c_\mu = \begin{cases} \dfrac{16}{\mathrm{Re}}, & \mathrm{Re} \leqslant 10.9; \\ \left(\dfrac{48}{\mathrm{Re}}\right)\left(1-\dfrac{2.2}{\sqrt{\mathrm{Re}}}\right), & \mathrm{Re} > 10.9; \end{cases}$$

where the bubble Reynolds number is defined as

$$\mathrm{Re} = \frac{2a\rho_L|u-u_G|}{\mu}$$

and μ is the liquid viscosity.

Define the intensity of the liquid vaporization into a bubble as j and the bubble-break-up intensity as ψ. Assuming that the bubbles streaming does not affect the process of vaporization,

$$j = 2\pi a D_L \rho_G \mathrm{Ja}\,\mathrm{Nu}$$

is obtained, where

$$\mathrm{Ja} = \frac{c_L\rho_L(T_L-T_s)}{\rho_L l}, \quad \mathrm{Nu} = \frac{2a}{T_L-T_s}\left.\frac{\partial T}{\partial r}\right|_{r=a}$$

are the Jacob and Nusselt numbers, c_L and D_L are the coefficients of heat and temperature conductivity, l is the specific heat of vaporization, T_L and T_s are the liquid and vapour temperatures and r is the polar radius of a spherical coordinate system with its centre at the bubble centre.

It is known (Scriven 1959) that if the liquid temperature is constant on its boundary with a bubble then, in the course of time, the temperature distribution around a bubble reaches the profile corresponding to an automodel solution. The profile occurs at time $\tau_T \sim (a/\mathrm{Nu})^2/D_L \sim 10^{-3}$ s. In time τ_T the liquid temperature changes on its boundary with a bubble by approx. 0.1 K, i.e. much less than characteristic liquid overheats which are ~ 10 K [figure 1(a)]. Therefore, the temperature distribution around a bubble is considered in order to satisfy the automodel solution at every moment in time. Since the ratio of the vapour density to that of the liquid is $\rho_G/\rho_L \ll 1$ for the flow under consideration, the approximation offered for this case by Labuntsov *et al.* (1964) is used:

$$\mathrm{Nu} = \frac{12}{\pi}\mathrm{Ja}\left[1+\frac{1}{2}\left(\frac{\pi}{6\,\mathrm{Ja}}\right)^{2/3}+\frac{\pi}{6\,\mathrm{Ja}}\right].$$

Bubble break-up occurs as a result of interphase surface instability. The hypothesis has been proposed and proved, with the help of known experimental data (Nigmatulin 1978), that the basic regularities for the development of instability in spherical surfaces are the same as for a plane interphase boundary.

The rise in amplitude of a harmonic perturbation with wavelength λ arising on a plane interphase boundary is given by (Birkhoff 1960):

$$\delta = \delta_0 \exp[I(\lambda)t], \quad [10]$$

where δ_0 is the amplitude of an initial perturbation,

$$I(\lambda) = \left[\frac{\rho_L \rho_G (u_G - u_L)^2 4\pi^2}{(\rho_L + \rho_G)^2 \lambda^2} - \frac{\Sigma 8\pi^3}{(\rho_L + \rho_G)\lambda^3} \right] \quad [11]$$

and Σ is the coefficient of surface tension.

The expression for I, [11], considers only Kelvin–Helmholtz instability, which arises from the difference in the phase velocities.

From [11], it follows that I will be positive ($I > 0$) when the wavelength of a harmonic perturbation is greater than a critical value:

$$\lambda > \frac{2\pi\Sigma(\rho_G + \rho_L)}{(\mu_G - u_L)^2 \rho_L \rho_G}. \quad [12]$$

On the other hand, according to Nigmatulin's scheme, the length of a wave causing bubble break-up cannot be greater than its diameter:

$$\lambda \leqslant 2a. \quad [13]$$

It follows from [12] and [13] that perturbation of a bubble surface occurs when Weber's number reaches its critical value, $We^* = 2\pi$:

$$We = \frac{2a(u_G - u_L)^2}{\Sigma} \frac{\rho_L \rho_G}{\rho_G + \rho_L} > 2\pi.$$

Bubble break-up occurs in the time t^* which is required for the amplitude of the perturbation to reach a value comparable with the bubble radius ($\delta \sim a$).

Since the amplitude of perturbations increases according to an exponential law [10], t^* is assessed as

$$t^* \sim \frac{1}{I(\lambda^*)},$$

where λ^* is the wavelength for which $1/I$ is minimal.

The expression for t^* is given by (Nigmatulin 1978)

$$t = \left[\frac{\rho_L a^3}{\Sigma} \left(\frac{We^*}{We} \right)^3 \right]^{1/2}.$$

Knowing the characteristic time of bubble break-up t^* and assuming that a bubble divides into two parts, an approximation can be made by the relaxation equation:

$$\psi = \begin{cases} 0, & \text{if } We < We^* = 2\pi; \\ (n^* - n)/t^*, & \text{if } We \geqslant We^*; \end{cases}$$

where n is the number of bubbles in a unit volume of the mixture and n^* is the number of bubbles in a unit volume of the mixture under the condition of an instantaneous break-up:

$$\frac{n^*}{n} = 2.$$

The numerical integration method is given in the Appendix.

3. RESULTS OF THE NUMERICAL CALCULATION

The efflux of boiling liquid from a semi-infinite channel is considered. This solution allows the exclusion of waves formed by reflection from the closed end of the vessel from the wave picture. The numerical calculation of this process within the bounds of the model considering bubble break-up that the wave configuration consists of three waves—schematically shown in figure 3 by the solid line. The configuration obtained when using the model (Nigmatulin & Soplenkov 1980) which does not consider bubble break-up is shown by the dotted line.

A fast wave of discharge, consisting of an elastic precursor, a "trough" of boiling and a zone

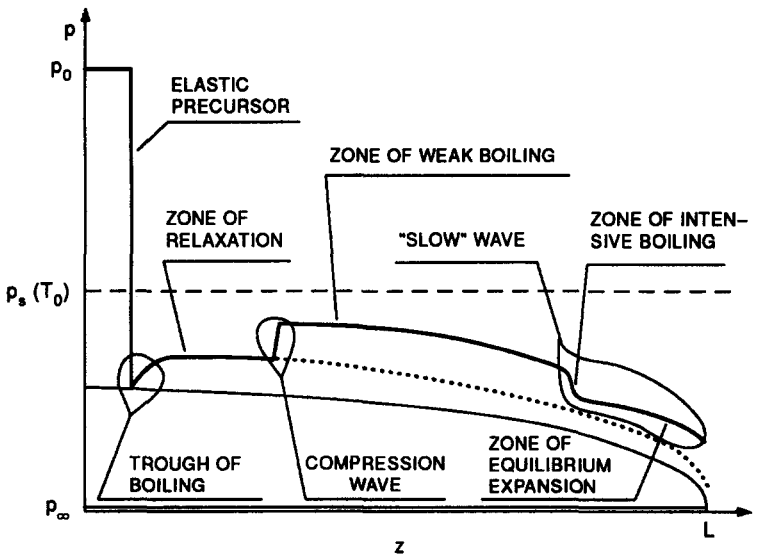

Figure 3. Scheme of the progression of the wave process after the opening of a semi-infinite channel: · · · ·, calculation with the model without bubble break-up; ——, calculation with the advanced model.

of relaxation, is the first move in the channel. The forefront of this wave, an elastic precursor spreading at the speed of sound in the liquid, converts the liquid into a metastable state.

After the passage of the elastic precursor the pressure in the mixture begins to increase rapidly but, in contrast to the case of a compression wave, the pressure growth is accompanied by an increase in the specific mixture volume. Gradually the pressure growth ceases and further liquid expansion proceeds under slowly decreasing pressure.

Near the exit cross-section of the vessel the bubble size, the pressure gradient, the stream acceleration and, consequently, the phase speed difference are at a maximum. The conditions for bubble break-up are created initially at the channel exit. Bubble break-up causes a sharp increase in the interphase area, which leads to intensification of the vaporization process.

An explosion-like boiling increases the pressure at the channel exit, and a compression wave recedes into the vessel after the discharge wave. A second discharge wave, in which three zones can be distinguished, follows the compression wave: (1) a zone of weak boiling, in which the non-equilibrium mixture is boiling on initial nucleation centres; (2) a zone of intensive boiling, in which the interphase mass exchange is intensified (due to bubble break-up) and the mixture is converted into a state of equilibrium; and (3) a zone of equilibrium expansion.

When the boiling liquid flows out of real constructions, vessels of finite length, the first wave of discharge reflects from the closed end of the tube and going back, it creates an area with an increased content of vapour and damping. When the compression wave passes through this area, it also causes damping and the pressure becomes uniform from the closed end of the tube to the front of the bubble break-up. The second wave of discharge degenerates into a "slow" wave. Thus, the "slow" wave of discharge noticed in experiments (Edwards & O'Brien 1970; Isaev 1980) is none other than part of the second wave of discharge or, in other words, the wave of reorganization of the second discharge wave profile.

The pressure distributions and number of bubbles per unit of mixture volume and the volumetric vapour content at different moments in time are shown in figure 4; the numbers in this diagram correspond to the time in seconds.

It is seen that bubble break-up leads to rapid growth of the volumetric vapour content (to the expansion of the mixture), a pressure fall and, consequently, to an increase in the difference in the phase velocities. The conditions for bubble break-up are created up to the flow.

The spread velocity of the front of bubble break-up and, consequently, this velocity of a "slow" wave movement are gradually increased. This is related to the fact that this wave is moving through the medium with an ever-increasing vapour content, while a vapour content increase in the mixture

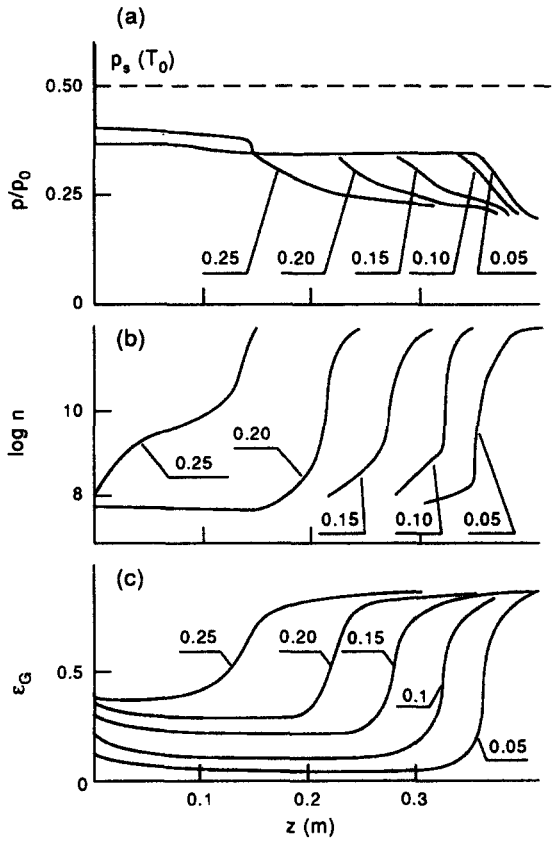

Figure 4. Parameter distribution along the channel under the motion of a "slow" wave of discharge. The numerals in the plot correspond to the process time in seconds.

facilitates the process of bubble break-up. At a sufficiently distant point of the tube, where the mixture transition into a state of equilibrium has time to occur without the destruction of bubbles, a "slow" discharge wave will regenerate into a centred discharge wave moving through the equilibrium mixture.

Pressure oscillograms at some points of the vessel, calculated on the advanced model, are shown in figure 1(c). Experimental and calculated oscillograms of the pressure and volumetric vapour content in the cross-section 1.39 m from the closed end of the tube are compared in figure 2(a,b). The results of the calculations with the given model are shown by a dash–dot line. It is seen that the advanced model permits the description of the efflux process both qualitatively and quantitatively.

4. THE EFFECT OF A FREE PARAMETER ON NUMERICAL CALCULATIONS OF THE BOILING LIQUID EFFLUX PROCESS

The only free parameter in the given model is the number of particles that nucleate boiling n_0. The parameter n_0 is chosen so that predicted overheats $(T_l - T_s)$ correspond to experimental ones in the initial stage of efflux ($t \leqslant 10^{-2}$ s). On these grounds, the value of n_0 is taken to be $10^8\ m^{-3}$. Choosing such an n_0, the main stage of the discharge process can be described ($t \sim 10^{-1}$ s).

Consider what will happen to the prediction if n_0 is either greater or smaller than $10^8\ m^{-3}$. When n_0 is taken to be too high, $10^{11}\ m^{-3}$, liquid and vapour, according to the given model, should be practically in equilibrium, due to the large interphase surface. In this case, the predictions of the given model coincide with that of an equilibrium model—shown by the dotted line in figure 2(a,b). As shown earlier this model does not describe the experiment.

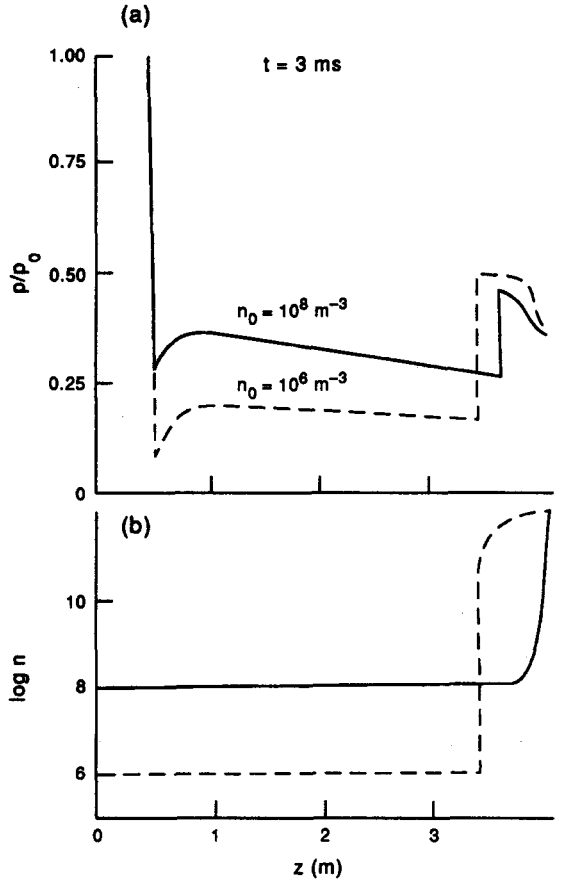

Figure 5. The effect of a free parameter on the numerical calculations of an initial stage of the boiling liquid efflux process: ——, $n_0 = 10^8\,\mathrm{m}^{-3}$; – – –, $n_0 = 10^6\,\mathrm{m}^{-3}$. (a) Pressure and (b) number of bubbles distributions along the channel at time $t = 3$ ms.

Compare the calculations of an initial efflux stage in two cases. In the first one, $n_0 = 10^8\,\mathrm{m}^{-3}$ (solid line in figure 5); and in the second one, $n_0 = 10^6\,\mathrm{m}^{-3}$ (dotted line in figure 5). It is seen that in the second case the compression wave has a greater amplitude and bubble break-up occurs in this wave (figure 5). As a result of break-up, the number of bubble increases by 6 orders of magnitude and the mixture transfers into an equilibrium state. Thus, calculations with a small number of initial nucleation centres predict that the mixture reaches equilibrium in the whole channel in time $t \lesssim 10^{-2}$ s, which falls short of the experimental data.

Therefore, the given model describes the experiment only for certain values of the number of initial nucleation centres $n_0 = 10^8\,\mathrm{m}^{-3}$.

5. CONCLUSIONS

In the present paper it has been shown that the difference in phase velocities cannot, in general, be neglected in the modelling of boiling liquid flows. Even a small difference in the phase velocities $|u_L - u_G| \ll u_L$ may cause bubble break-up. An increase in the number of bubbles may, in turn, initiate shock waves and "slow" waves of discharge.

REFERENCES

BATCHELOR, G. K. 1970 *An Introduction to Fluid Dynamics*. Cambridge Univ. Press, Cambs.

BIRKHOFF, G. 1960 *Hydrodynamics*. Princeton Univ. Press, Princeton, N.J.

BRABSTON, D. C. & KELLER, H. B. 1975 Viscous flows past spherical gas bubbles. *J. Fluid Mech.* **69,** 179–189.

EDWARDS, A. R. & O'BRIEN, T. P. 1970 Studies on phenomena connected with the depressurization of water reactors. *J. Br. Nucl. Engng Soc.* **9,** 125–135.

GODUNOV, C. K. & RIYABENKII, V. C. 1973 *Differential Schemes*. Nauka, Moscow (in Russian).

ISAEV, O. A. 1980 Liquid boiling under a fast pressure fall in an adiabatic unsteady stream. Author's essay of a candidate dissertation, Sverdlovsk (in Russian).

IVANDAEV, A. I. & GUBAIDULLIN, A. A. 1978 The investigation of an unsteady efflux of boiling liquid in a thermodynamic-equilibrium approximation. *High Temp. Heat-Phys.* **18,** 556–562.

LABUNTZOV, D. A. & AVDEEV, A. A. 1981 The boiling jump theory. *High Temp. Heat-Phys.* **19,** 552–556.

LABUNTSOV, D. A., KOLSCHYGIN, B. A., ZACHAROVA, E. A. & VLADIMIROVA, L. N. 1964 The study of bubble growth under the boiling of saturated water in a wide range of pressure changes with the help of rapid filming. *High Temp. Heat-Phys.* **2,** 446–453.

NIGMATULIN, B. I. & SOPLENKOV, K. I. 1980 The study of an unsteady efflux of boiling liquid from channels in a thermodynamic non-equilibrium approximation. *High Temp. Heat-Phys.* **18,** 118–131.

NIGMATULIN, R. I. 1978 *Foundations of Mechanics of Heterogeneous Media*. Nauka, Moscow (in Russian).

RICHTMYER, R. D. & MORTON, K. V. 1967 *Difference Methods for Initial-value Problems*. Interscience, New York.

SCRIVEN, L. E. 1959 On the dynamics of phase growth. *Chem. Engng Sci.* **10,** 1–13.

APPENDIX

Numerical Procedures

Equations [1]–[5] may be written in the form

$$\frac{\partial}{\partial t}[\mathbf{U}] + \frac{\partial}{\partial z}[\mathbf{F}(\mathbf{U})] = \mathbf{J}(\mathbf{U}), \qquad [A.1]$$

where

$$\mathbf{U} = \begin{Bmatrix} \rho \\ \rho_G \epsilon \\ \rho u \\ \rho(i + u^2/2) - p \\ n \end{Bmatrix}, \quad \mathbf{F} = \begin{Bmatrix} \rho u \\ \rho_G \epsilon u \\ \rho u^2 + p \\ \rho u(i + u^2/2) \\ nu \end{Bmatrix}, \quad \mathbf{J} = \begin{Bmatrix} 0 \\ jn \\ 0 \\ 0 \\ \psi \end{Bmatrix}$$

are the vector parameters.

The method of numerical integration of these equations is constructed on the basis of a two-step Lax–Wendroff scheme (Richtmyer & Morton 1967).

The method of Lax–Wendroff can be applied for the integration of equations which have no source terms ($\mathbf{J} = 0$). For integration of the set of equations [A.1] containing source terms the method of splitting on a physical parameter is used (Godunov & Riyabenkii 1973). This method applied to the given system consists of the following: at first vector $\mathbf{U}'$ is calculated ignoring source terms, then, using $\mathbf{U}'$, we determine the source terms $\mathbf{J}(\mathbf{U}')$ with the help of which we define $\mathbf{U}$.

The numerical scheme constructed by this method is:

first step,

$$(\mathbf{U}')_{j+1/2}^{n+1/2} = \tfrac{1}{2}(\mathbf{U}_{j+1}^{n} + \mathbf{U}_{j}^{n}) - \frac{\Delta t}{2\,\Delta z}(\mathbf{F}_{j+1}^{n} - \mathbf{F}_{j}^{n});$$

second step,

$$\mathbf{U}_{j+1/2}^{n+1/2} = (\mathbf{U}')_{j+1/2}^{n+1/2} + \frac{\Delta t}{2}\mathbf{J}((\mathbf{U}')_{j+1/2}^{n+1/2});$$

third step,

$$(\mathbf{U}')_{j}^{n+1} = \mathbf{U}_{j}^{n} - \frac{\Delta t}{\Delta z}(\mathbf{F}_{j+1/2}^{n+1/2} - \mathbf{F}_{j-1/2}^{n+1/2});$$

fourth step,

$$\mathbf{U}_{j}^{n+1} = (\mathbf{U}')_{j}^{n+1} + \Delta t\,\mathbf{J}((\mathbf{U}')_{j}^{n+1}).$$

[A.2]

Since [6] cannot be represented in the form [A.1], it is integrated using the other scheme. Equation [6] is represented with the closing ratios [7]–[9] in a form more convenient for numerical integration. Taking the ratio of vapour density/liquid density as being small, $\rho_G/\rho_L \ll 1$,

$$\frac{\partial[\rho u_G]}{\partial t} + \frac{\partial[\rho u u_G]}{\partial z} = \frac{\partial[3\rho u]}{\partial t} + \frac{\partial[3\rho u^2]}{\partial z} - 3(u_G - u)(1-\epsilon)\left\{\frac{\partial[\rho \ln a]}{\partial t} + \frac{\partial[\rho u \ln a]}{\partial z}\right\} + I \quad [A.3]$$

is obtained, where

$$I = \frac{3\epsilon(1-\epsilon)j}{4\pi a^3}(u - u_G) + \frac{3\rho c_\mu}{4a}(u - u_G)|u - u_G|.$$

To write the numerical scheme in a more compact form, two numerical operators are introduced:

$$L(A)_{j+1/2}^{n+1/2} = A_{j+1/2}^{n+1/2} - \tfrac{1}{2}(A_{j+1}^{n} + A_{j}^{n}) + \frac{\Delta t}{2\,\Delta t}[(uA)_{j+1}^{n} - (uA)_{j}^{n}]$$

and

$$L(A)_{j}^{n+1} = A_{j}^{n+1} - A_{j}^{n} + \frac{\Delta t}{\Delta z}[(uA)_{j+1/2}^{n+1/2} - (uA)_{j-1/2}^{n+1/2}],$$

where A is any parameter of the system.

The numerical scheme for the integration of [A.3] is:

first step,

$$(\rho' u')_{j+1/2}^{n+1/2} = \tfrac{1}{2}[(\rho u_G)_{j+1}^{n} + (\rho u_G)_{j}^{n}] - \frac{\Delta t}{2\,\Delta z}[(\rho u u_G)_{j+1}^{n} - (\rho u u_G)_{j}^{n}] + L(3\rho' u')_{j+1/2}^{n+1/2}$$
$$- \tfrac{3}{2}[\{(u_G - u)(1-\epsilon)\}_{j+1}^{n} + \{(u_G - u)(1-\epsilon)\}_{j}^{n}]L(\rho' \ln a')_{j+1}^{n+1}$$

second step,

$$(\rho u_G)_{j+1/2}^{n+1/2} = (\rho' u_G')_{j+1/2}^{n+1/2} + \frac{\Delta t}{2} I((\mathbf{U}')_{j+1/2}^{n+1/2}, (\rho' u_G')_{j+1/2}^{n+1/2});$$

third step,

$$(\rho' u')_{j}^{n+1} = (\rho u)_{j}^{n} - \frac{\Delta t}{\Delta z}[(\rho u u_G)_{j+1/2}^{n+1/2} - (\rho u u_G)_{j-1/2}^{n+1/2}]$$
$$+ L(3\rho' u')_{j}^{n+1} - 3\{(u_G - u)(1-\epsilon)\}_{j}^{n} L(\rho' \ln a')_{j}^{n+1};$$

fourth step,

$$(\rho u_G)_{j}^{n+1} = (\rho' u_G')_{j}^{n} + \Delta t I((\mathbf{U}')_{j}^{n+1}, (\rho' u_G')_{j}^{n+1}).$$

[A.4]

Consider the sequence of operations to integrate the set of equations [1]–[5] and [A.3] on schemes [A.2] and [A.4]. The values $u_{j+1/2}'^{n+1/2}$, $\rho_{j+1/2}'^{n+1/2}$ and $a_{j+1/2}'^{n+1/2}$, which are preliminarily defined by integrating [1]–[5] in the first step of scheme [A.2], come into the operators $L_{j+1/2}^{n+1/2}$ used in the first

step of scheme [A.4]. Therefore, the first step of scheme [A.4] should follow the first step of scheme [A.2].

Analogously, the operators L_j^{n+1} used in the third step of scheme [A.4] contain the values $u_j'^{n+1}$, $\rho_j'^{n+1}$ and $a_j'^{n+1}$, which are determined after the third step of scheme [A.2] has been performed. Therefore, the third step of scheme [A.4] should follow the third step of scheme [A.2].